



1 **Molecular Composition and Photochemical Evolution of Water**
2 **Soluble Organic Carbon (WSOC) Extracted from Field Biomass**
3 **Burning Aerosols using High Resolution Mass Spectrometry**

4

5 Jing Cai^{1,2}, Xiangying Zeng¹, Guorui Zhi³, Sasho Gligorovski¹, Guoying Sheng¹,
6 Zhiqiang Yu^{1,*}, Xinming Wang¹, Ping'an Peng¹

7

8 ¹*State Key Laboratory of Organic Geochemistry, Guangdong Key Laboratory of*
9 *Environment and Resources, Guangzhou Institute of Geochemistry, Chinese*
10 *Academy of Sciences, Guangzhou, 510640, China*

11 ²*University of Chinese Academy of Sciences, Beijing, 100049, China*

12 ³*State Key Laboratory of Environmental Criteria and Risk Assessment, Chinese*
13 *Research Academy of Environmental Sciences, Beijing, 100012, China*

14

15 *corresponding author: Dr. Zhiqiang Yu

16 Tel: +86-13728068752

17 Fax: +86-20-85290288

18 E-mail: zhiqiang@gig.ac.cn

19

20

21

22

23

24



25 **ABSTRACT**

26 Photochemistry plays an important role in the evolution of atmospheric water
27 soluble organic carbon (WSOC), which dissolves into clouds, fogs and aerosol liquid
28 water. In this study, we examined the molecular composition and evolution of a
29 WSOC mixture extracted from fresh biomass burning aerosols upon photolysis,
30 using direct infusion electrospray ionization high-resolution mass spectrometry
31 (ESI-HRMS) and liquid chromatography coupled with mass spectrometry
32 (LC/ESI-HRMS). For comparison, two typical phenolic compounds (i.e., phenol and
33 guaiacol) emitted from lignin pyrolysis in combination with hydrogen peroxide
34 (H₂O₂) as a typical OH radical precursor, were exposed to simulated sunlight
35 irradiation. The photochemistry of both, the phenols (photo-oxidation) and WSOC
36 mixture (direct photolysis) can produce a series of highly oxygenated compounds
37 which in turn increases the degree of oxidation of organic composition and acidity of
38 the bulk solution. In particular, the LC/ESI-HRMS technique revealed significant
39 photochemical evolution on the WSOC composition, e.g., the photodegradation of
40 low oxygenated species and the formation of highly oxygenated products. We also
41 tentatively compared the mass spectra of photolytic time-profile extract with each
42 other for a more comprehensive description of the photolytic evolution. The
43 calculated average oxygen-to-carbon (O/C) ratios of oxygenated compounds in bulk
44 extract increases from 0.38 ± 0.02 to 0.44 ± 0.02 (mean \pm standard deviation) while
45 the intensity (S/N)-weighted average O/C (O/C_w) increases from 0.45 ± 0.03 to 0.53
46 ± 0.06 as the time of irradiation extends from 0 to 12h. These findings indicate that



47 the water soluble organic fraction of fresh combustion-derived aerosols have the
48 potential to form more oxidized organic matter, accounting for the highly
49 oxygenated nature of atmospheric organic aerosols.

50 1 INTRODUCTION

51 Water-soluble organic carbon (WSOC) comprises a significant fraction of
52 atmospheric aerosols, accounting for 20–80% of total organic carbon (OC) (Krivacsy
53 et al., 2001; Wozniak et al., 2008; Fu et al., 2015; Xie et al., 2016). WSOC is directly
54 involved in the formation of cloud condensation nuclei (CCN) by modifying the
55 aqueous chemistry and surface tension of cloud droplets (Graham et al., 2002;
56 Nguyen et al., 2012; Zhao et al., 2013; McNeill 2015). Despite its significance, little
57 is known about the chemical composition and sources of WSOC, with less than
58 10–20% of the organic mass being structurally identified (Cappiello et al., 2003; Fu
59 et al., 2015). Biomass burning is a well-known emission source of WSOC (Anastasio
60 et al., 1997; Fine et al., 2001; Graham et al., 2002; Mayol-Bracero et al., 2002;
61 Gilardoni et al., 2016). Although the composition varies with fuel type and
62 combustion conditions (Simoneit 2002; Smith et al., 2009), the WSOC mixture often
63 covers a common range of polar and oxygenated aromatic compounds (Graham et al.,
64 2002; Mayol-Bracero et al., 2002; Duarte et al., 2007; Chang and Thompson 2010;
65 Yee et al., 2013; Gilardoni et al., 2016) with molecules incorporating different
66 numbers of functional groups like COOH, C=O, CHO, COH, COC, CONO₂, CNH,
67 and/or CONH₂ groups (Graham et al., 2002). In particular, lignin pyrolysis often
68 yields a large amount of aromatic alcohols, carbonyl, and acid compounds



69 (Mayol-Bracero et al., 2002; Chang and Thompson 2010; Gilardoni et al., 2016).
70 Once dissolved into cloud, fog, and even aerosol liquid water, these substances can
71 undergo aqueous-phase reactions to affect aerosol evolution processes under sunlight
72 irradiation, and produce low-volatility species, which have the potential to form
73 secondary organic aerosol (SOA) after water evaporation (Graham et al., 2002;
74 Cappiello et al., 2003; Duarte et al., 2007; Sun et al., 2010; Yu et al., 2014).

75 Field and laboratory studies have demonstrated that aqueous photochemical
76 processes contribute significantly to the aqueous SOA formation from biomass
77 burning precursors and the evolution of smoke particles (Sun et al., 2010; Lee et al.,
78 2011; Kitanovski et al., 2014; Yu et al., 2014; McNeill 2015; Gilardoni et al., 2016).
79 Gilardoni et al. (2016) observed aqueous SOA formation in both fog water and wet
80 aerosols, resulting in an enhancement in the oxidized OA, and following
81 atmospheric aging the overall O/C ratios of aerosols has also increased. In laboratory
82 studies, phenols and methoxyphenols (important biomass burning emerged
83 intermediates) are often used as SOA precursors to examine the photochemical
84 evolution in aqueous environment and aerosol-forming potential under relevant
85 atmospheric conditions (Chang and Thompson 2010; Sun et al., 2010; Smith et al.,
86 2014; Yu et al., 2014, Vione et al., 2019). The corresponding photochemical products
87 formed through hydroxylation, oligomerization, and fragmentation typically cover a
88 series of low-volatility and highly oxygenated species. For instance, the
89 methoxyphenol-derived SOA are proposed as a proxy for atmospheric humic-like
90 substances (HULIS) (Ofner et al., 2011; Yee et al., 2013). Other compounds emitted



91 from lignin pyrolysis, e.g., aromatic alcohol, carbonyl, and carboxylic species
92 retaining the phenyl ring have also been found to produce colored products via
93 aqueous photo-oxidation, which may become a part of HULIS (Chang and
94 Thompson 2010, Huang et al., 2018). In addition, photochemical processing of
95 common water-soluble aliphatic compounds such as aldehydes (Lim and Turpin
96 2015), polyols (Daumit et al., 2014), and organic acids (Griffith et al., 2013) in
97 aqueous solution can also lead to the formation of oligomers, highly oxygenated and
98 multifunctional organic matter (McNeill 2015).

99 In recent years, high resolution mass spectrometry (HRMS) has been commonly
100 applied to study the organic molecular composition in cloudwater (Zhao et al., 2013;
101 Boone et al., 2015), fogwater (Cappiello et al., 2003), rainwater (Altieri et al., 2009a;
102 Altieri et al., 2009b), laboratory-generated SOA (Bateman et al., 2011; Romonosky
103 et al., 2015; Lavi et al., 2017), and field-collected aerosol samples (Laskin et al.,
104 2009; Lin et al., 2012a; Lin et al., 2012b; Kourtchev et al., 2013). It has also been
105 used in time-profile observations of the photochemical evolution of aqueous extracts
106 from laboratory-generated SOAs (Bateman et al., 2011; Romonosky et al., 2015).
107 However, direct infusion MS methods are prone to ion suppression caused by other
108 organic species, inorganic salts, and adduct formation (Kourtchev et al., 2013).
109 Therefore, HRMS coupled with LC might be another complementary powerful tool
110 for relieving ion suppression (Kourtchev et al., 2013; Wang et al., 2016). It could
111 also provide more information enabling the identification of possible isomers from
112 the ions with same mass-to-charge ratio (m/z).



113 To our knowledge, the aqueous photochemical evolution of WSOC extracted from
114 real ambient aerosols has not been studied in detail at the molecular level. The
115 present study is focused on a further analysis of the previously studied field collected
116 samples by Cai et al. (2018). Here, the main goal is to investigate the molecular
117 characteristics of water-soluble organic molecules by the photochemical evolution
118 using ESI-HRMS and LC/ESI-HRMS performed in negative ionization mode. The
119 photochemistry of phenol and guaiacol was evaluated under laboratory conditions as
120 well, and used as a reference.

121 **2 EXPERIMENTAL SECTION**

122 **2.1 Particulate sample collection and preparation of aqueous extracts**

123 Fresh straw-burning aerosols were collected during the summer harvest season of
124 2013, at rural fields in north China (Cai et al., 2018). Briefly, the selected samples
125 used for HRMS analysis were collected from two sampling sites, located at rural
126 fields in Wenxian in Henan Province (noted: HNWX) and Daming county in Hebei
127 Province (HBDM). The selected sampling sites were mainly affected by heavy smog
128 from straw burning (Figure 1). As described in Cai et al. (2018), particulate matter
129 ($\leq 2.5\mu\text{m}$) was sampled by a portable particulate sampler (MiniVol TAS, AirMetrics,
130 USA), with quartz filters (47mm in diameter, QMA, Whatman, UK) baked at 600°C
131 for 6 hours before sampling.

132 The preparation of straw-burning particle extracts and measurements for carbon
133 content including organic carbon (OC), elemental carbon (EC) and WSOC were



134 described in detail in Cai et al. (2018). A pH meter (Mettler Toledo SevenEasy™
135 S20) calibrated at pH 4.00 and 6.86 was applied for extract pH measurements. Prior
136 to analysis the extract solutions were stored at -20°C in the dark. To reduce the
137 WSOC mass loss, the desalting treatment (e.g., solid phase extraction (SPE)) was not
138 performed on these samples.



Figure 1. One field site at Daming, Hebei province, China, for sampling the aerosols affected by biomass burning.

148 2.2 Laboratory observation of the direct photolysis of WSOC extracts

149 A 12-hour direct photolysis of particle extracts was performed in a photoreactor
150 (BL-GHX-V, Bilon Instruments Co. Ltd., China, see Figure S1) (Cai et al., 2018). In
151 the wavelength range of 310-400 nm relevant to the boundary layer of the
152 atmosphere, the actinic flux of the lamp is about 5 times stronger than the solar
153 actinic flux, meaning that the spectral evolution via the 12-hour simulated solar
154 irradiation might be equal with the effect caused by actual sunlight irradiation with a



155 duration of at least 60 hours. As described in Cai et al. (2018), the water extraction
156 resulted in a dilution of the collected organic compounds, however, the ratio of the
157 water mass to PM_{2.5} mass for extraction was compatible with the ratio of water mass
158 to WSOC content in cloud water, indicating that the present aqueous extracts are
159 relevant to the atmospheric cloud water condition (Li et al., 2017).

160 In the experimental section of phenol photochemistry, initial solution of 0.1 mM
161 phenol and 0.1 mM guaiacol in combination with an OH radical precursor (0.1 mM
162 H₂O₂), were prepared in ultra-pure water (Milli-Q, Milipore). The pH of the solution
163 was adjusted to 5 with 0.1 M sulfuric acid (H₂SO₄), which is usually relevant to the
164 acidity in fog and cloud waters (Collet et al., 1998, Fahey et al., 2005). The prepared
165 solution and reference blank were irradiated by simulated sunlight irradiation with a
166 duration of 4 hours. Hereby, we mainly focus on acquiring the chemical
167 characteristics of aqueous products of phenols, and tentatively identify some
168 biomarkers (e.g., phenolic dimers) whether they exist in the real biomass burning
169 particulate samples.

170 **2.3 Sample analysis**

171 The direct infusion MS analysis was conducted using a Thermo Scientific
172 Orbitrap Fusion Tribrid mass spectrometer equipped with a quadrupole, orbitrap, and
173 linear ion trap mass analyzers, with a heated ESI source. To assist in ionization and
174 desolvation, the aqueous extract was diluted to a 1:1 mixture of acetonitrile and
175 sample by volume. The full scan mass spectra were acquired in negative ionization
176 mode, with a resolution of 120 000 at *m/z* 200 for the orbitrap analyzer and a mass



177 scan range of m/z 50-750. Before determination, the orbitrap analyzer was externally
178 calibrated for mass accuracy using Thermo Scientific Pierce LTQ Velos ESI
179 calibration solution. The direct infusion parameters were as follows: sample flow
180 rate $5\mu\text{l min}^{-1}$; capillary temperature 300°C ; S-lens RF 65%; spray voltage -3.5kV;
181 sheath gas, auxiliary gas, and sweep gas flows were 10, 3, and 0 arbitrary units,
182 respectively. Data collecting was performed when the intensity of the total ion
183 current (TIC) maintained constant with an $\text{RSD} < 5\%$. At least 100 data points (mass
184 spectral scans) were collected for each test sample, and the each exported mass
185 spectra for analysis was derived from the average result of 100 spectrums.

186 The LC/ESI-HRMS analysis operated in negative ionization mode was performed
187 using a U3000 system coupled with a T3 Atlantis C18 column ($3\mu\text{m}$; $2.1 \times 150\text{mm}$;
188 Waters, Milford, USA) and an Orbitrap Fusion MS. A $10\mu\text{L}$ extract was injected,
189 with a flow rate of 0.2 ml min^{-1} for the mobile phase, which consisted of H_2O (A)
190 and acetonitrile (B). The gradient applied was 0-5 min 3% B; 5-20 min from 3 to 95%
191 (linear), and kept for 25 min at 95%; and 45-50 min from 95 to 3%, and held for 10
192 min at 3% (total run time 60 min).

193 **2.4 Data processing**

194 Mass spectral peaks with three times larger than the signal to noise ratio (S/N)
195 were extracted from the raw files. Peaks in both sample and blank spectra were
196 retained if their intensity in the former was five times larger than in the latter. A
197 molecular assignment based on the accurate mass was performed using Xcalibur
198 software (V3.0 Thermo Scientific) with the following constraints: $^{12}\text{C} \leq 50$, $^{13}\text{C} \leq 1$,



199 $^1\text{H} \leq 100$, $^{16}\text{O} \leq 50$, $^{14}\text{N} \leq 4$, $^{32}\text{S} \leq 1$, and $^{34}\text{S} \leq 1$. All mathematically possible elemental
200 formulas, with a mass tolerance of ± 3 ppm were calculated. Elemental formulas
201 containing ^{13}C or ^{34}S were checked for the presence of ^{12}C or ^{32}S counterparts,
202 respectively. If they were not matched with the corresponding monoisotopic
203 formulas, then the assignment with next larger mass error was considered. Isotopic
204 and unassigned peaks were excluded from further analysis.

205 Ions were also characterized by the number of rings plus double bonds (i.e.,
206 double bond equivalents (DBE)), which were calculated as: $\text{DBE} = c - h/2 + n/2 + 1$ for
207 an elemental composition of $\text{C}_c\text{H}_h\text{O}_o\text{N}_n\text{S}_s$. The assigned formula was additionally
208 checked with the nitro-rule. For ambient samples, based on the presence of various
209 elements in a molecule, the identified elemental formulas were classified into several
210 main compound classes: CHO (i.e., molecules containing only C, H, and O atoms),
211 CHOS, CHON, and CHONS, and others including CHN and CHS. In the present
212 study, because the detected water-soluble ions almost were below m/z 400, we
213 focused our molecular analysis on m/z 50-400.

214 3 RESULTS AND DISCUSSION

215 3.1 Mass spectral characteristics of WSOC in biomass burning particulate

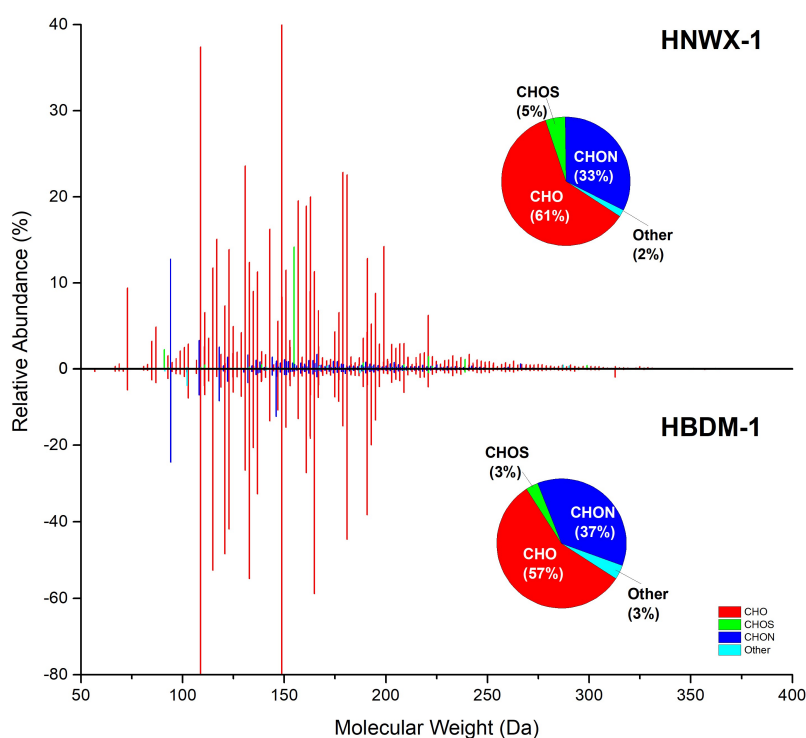
216 The $\text{PM}_{2.5}$ concentration in present straw burning smoke samples ranges from
217 6.46 to 28.03 mg m^{-3} (Table S1). OC is the major component of the collected $\text{PM}_{2.5}$
218 with a proportion of $50.9 \pm 7.6\%$ (mean \pm standard deviation), whereas EC
219 represents a negligible fraction (average $1.3 \pm 0.4\%$). Meanwhile, WSOC accounts
220 for $35.5 \pm 7.5\%$ of OC in the tested samples.



221 Four extract samples (HNWX-1, HNWX-2, HBDM-1 and HBDM-2) (Table S1)
222 analyzed using high resolution mass spectrometry showed similar patterns in mass
223 distribution of water-soluble molecular species that mainly range from 50 to 400 Da.
224 A group of reconstructed mass spectrum (abstracted blank) for two representative
225 samples HNWX-1, and HBDM-1 is shown, as an example, in Figure 2. In mass
226 range 50-400 Da, there were 827 ± 44 molecular formulas identified throughout the
227 all samples, and most of the formulas (above 75%) were overlapped between these
228 analyzed samples. The classification features of assigned compounds for analyzed
229 extracts are shown in Table S2. In the assigned formulas, CHO compounds were the
230 most abundant group, accounting for $59.2 \pm 2.2\%$ of the total assignments, followed
231 by CHON ($35.0 \pm 2.2\%$). These results are consistent with previous observations of
232 laboratory-generated biomass burning aerosol (Smith et al., 2009) and field
233 particulate samples influenced by biomass combustion (Kourtchev et al., 2016),
234 although the differences of biomass varieties, extracted solvent, and HRMS
235 techniques between present and previous studies. On the other hand, CHOS and
236 CHONS compounds contributed with less than 5% to the total assignment. A number
237 of studies have shown the wide presence of organosulfates and
238 nitrooxy-organosulfates in urban (Lin et al., 2012b; Wang et al., 2016), rural (Lin et
239 al., 2012a), and forest aerosols (Kourtchev et al., 2013), and even in cloudwater
240 (Boone et al., 2015); however, most of these compounds were not observed in our
241 negative mass spectra. This could be accounted for by the low extent of aerosol
242 evolution, due to the limited oxidation conditions available for the formation of



243 organosulfates and nitrooxy-organosulfates in fresh smoke aerosols. For example,
244 laboratory studies have observed the significant formation of organosulfates via
245 photooxidation in the presence of acidic sulfate aerosol (with significant level of SO₂
246 concentration) (Surratt et al., 2007; Surratt et al., 2008). All detected ion species with
247 enabled formula assignments in present samples are listed in Table S3.



248
249 **Figure 2. Reconstructed mass spectra of HNWX-1 and HBDM-1 sample. The inset pie**
250 **charts show the number fraction of each class in the total assigned compounds.**
251

252 The negative ion mode is prone for the detection of molecules containing polar
253 functional groups (e.g., -OH and -COOH). It should be noted that the formula
254 numbers detected in the HRMS potentially contain multiple structural isomers;

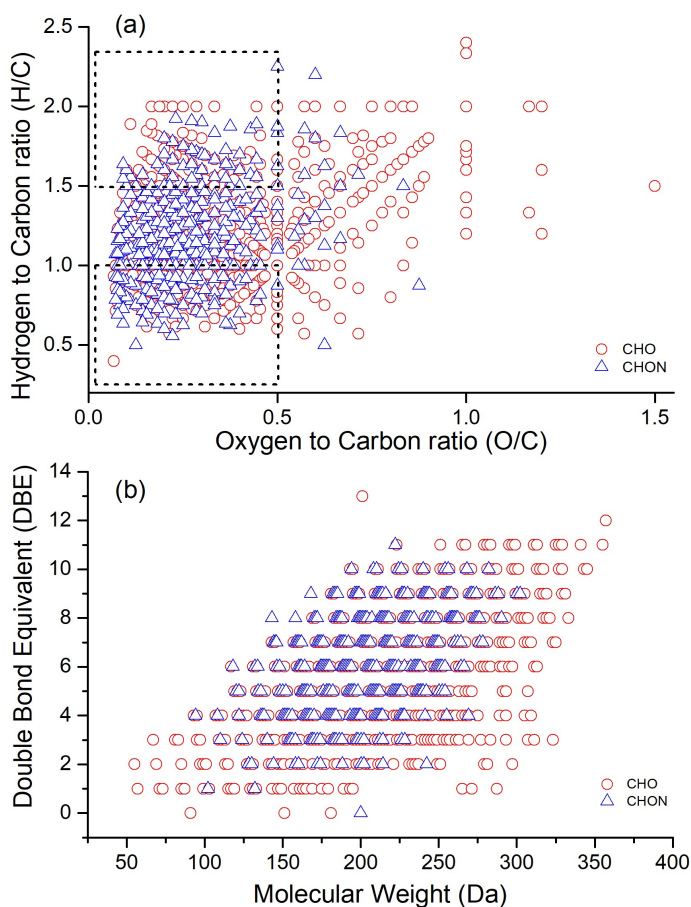


255 therefore, the actual number of water-soluble organic species might be
256 underestimated. The additional LC/ESI-HRMS analysis operated in negative mode
257 confirmed a substantial number of ion masses (e.g., assigned CHO and CHON
258 compounds) containing more than one structural isomer, which could be observed at
259 different retention times (RTs) in chromatograms. Two representative groups of
260 extracted chromatograms for CHO ($[C_7H_5O_n]^-$, (n=2~4)) and CHON ($[C_7H_5O_nN]^-$,
261 (n=1~3)) compounds are shown in Figure S2 and S3, respectively, where increasing
262 the O or N atom number in a molecule might lead to more isomer peaks. However, it
263 should be noted that these LC-separated peaks might also include other unidentified
264 compounds that were outside of the elemental assignment considered in this study.
265 Additionally, low content and potential decomposition under the ionization can also
266 limit the detection of some high molecular weight species.

267 The interpretation of the complex organic mass spectra generated by high
268 resolution mass spectrometry can be simplified by plotting the hydrogen to carbon
269 ratio(H/C) against the oxygen to carbon ratio (O/C) for individual assigned atomic
270 formulas in form of the Van Krevelen (VK) diagram (e.g. Lin et al., 2012a;
271 Kourtchev et al., 2013). Figure 3a indicates a representative VK diagram of CHO
272 and CHON compounds derived from HBDM-1 sample. It can be clearly seen from
273 Figure 3a that the majority of CHO and CHON molecules are located at the region of
274 $O/C \leq 1.0$ and $H/C \leq 2.0$. In VK diagram, molecules with $H/C \leq 1.0$ and $O/C \leq 0.5$
275 are typical for aromatic species, while molecules with $H/C \geq 1.5$ and $O/C \leq 0.5$
276 would be associated with typical aliphatic compounds (Mazzoleni et al., 2012;



277 Kourtchev et al., 2014). The average double bond equivalent (DBE) showed relative
278 high values with 5.5 for CHO compounds and 6.1 for CHON compounds (Table S2),
279 suggesting that oxidized aromatic compounds were abundant in the present sample,
280 and their presence could partially account for the strong light-absorbing feature in
281 the near-UV region as observed in our previous study (Cai et al., 2018). Figure 3b
282 shows the distribution of molecular formulas with various DBE and indicates a large
283 number of molecular species with high unsaturation degree ($\text{DBE} \geq 4$).



284
285 **Figure 3.** VK diagram (a) and DBE vs. molecular weight (b) of CHO and CHON
286 compounds for one representative sample (HNDM-1).



287 The average H/C and O/C ratios throughout the all extract samples were in the
288 ranges of 1.26-1.31 and 0.34-0.42 for CHO compounds, 1.19-1.23 and 0.28-0.29 for
289 CHON compounds (shown in Table S2), respectively. Although the ESI analysis
290 were performed in the negative ionization mode, the emerged O/C ratios exhibit
291 rather low values, which fall in the range of O/C ratios typical for biomass burning
292 organic aerosol derived from positive ionization mode (Aiken et al., 2008;
293 Kourtchev et al., 2016). Due to fresh emission and smaller aging effect, the present
294 O/C were obviously lower than the O/C of long-range transport biomass burning
295 aerosols (Zhang et al., 2018).

296 Carbon oxidation state (OS_c) was observed to increase with oxidation for
297 atmospheric organic aerosol and link strongly to aerosol volatility (Kroll et al., 2011).
298 OS_c for each molecular formula can be calculated using the following equation:

$$OS_c = - \sum_i OS_i \frac{n_i}{n_c}$$

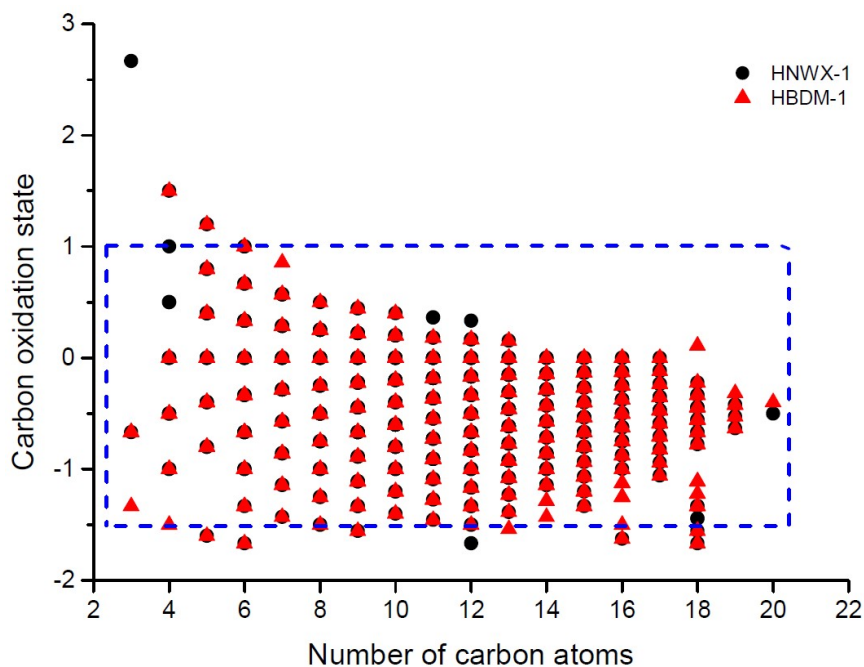
299 where OS_i is the oxidation state associated with element i and n_i/n_c is the molar ratio
300 of element i to carbon within the molecule (Kroll et al., 2011; Kourtchev et al., 2013).

301 Figure 4 shows an overlap in OS_c plots of CHO compounds for two representative
302 samples (HNWX-1 and HBDM-2) derived from different sampling sites. It can be
303 seen that OS_c ranges mainly from -1.5 to +1 with an average of 0.4. Consistent with
304 previous studies (Kroll et al., 2011; Kourtchev et al., 2016), the majority of molecules
305 with $OS_c < 0$ (low oxidized organics) and carbon atoms (n_c) lower than 20 are
306 suggested to be associated with the primary organic aerosols emitted from biomass
307 burning. A minor fraction of molecular formulas with $OS_c \geq 0$ values might be



308 associated with semivolatile and low-volatility oxidized organic aerosols (Kroll et al.,
309 2011).

310 A similar trend of OS_c values versus carbon number was obtained in previous
311 studies focused on the molecular composition of organic aerosols in urban area (Wang
312 et al., 2017) and at a road tunnel site (Tong et al., 2016), although the formulas of the
313 specific molecular products observed from different precursors in both studies are
314 quite different.



315

316 **Figure 4.** Carbon oxidation state (OS_c) vs. number of carbon atoms in CHO molecules.

317 3.2 Photochemical oxidation of phenols under laboratory conditions

318 Phenol and guaiacol were chosen as two representative model compounds derived
319 from biomass combustion. Two high resolution mass spectra of aqueous phenol and



320 guaiacol exposed to OH radicals for 4h, are shown in Figure S4. In Figure S4, 435
321 $C_xH_yO_z$ molecular formulas (m/z 90-500) were assigned for product ions of phenol
322 (with C_3 - C_{24}), whereas 624 $C_xH_yO_z$ formulas (m/z 90-600) were assigned for product
323 ions of guaiacol (with C_3 - C_{27}). The average H/C and O/C ratios were 0.79 ± 0.28 and
324 0.52 ± 0.23 for phenol, and 0.88 ± 0.24 and 0.59 ± 0.24 for guaiacol, respectively.
325 Clearly, the photochemical processing induced by OH oxidation resulted in an
326 increase in O/C of product molecules relative to their precursors (O/C=0.17 for
327 phenol and O/C= 0.29 for guaiacol). Meanwhile, the average OS_C of products for
328 phenol ($OS_C = -0.7$) and guaiacol ($OS_C = -0.6$) photooxidation were +0.2 and +0.3,
329 respectively, showing an increase with oxidation. The later implies that potentially
330 the phenols and methoxyphenols might undergo photochemical aging and thus alter
331 the nature of primary organic aerosols (Huang et al., 2018).

332 The formation mechanisms of series of oxygenated products, e.g., phenolic
333 oligomers, hydroxylated phenolic species, ring-opening and highly oxygenated
334 compounds, are proposed in the literature (e.g. Sun et al., 2010; Chang and
335 Thompson, 2010, Yu et al., 2014). The OH-initiated reactions would result in
336 enhanced hydroxylation of the aromatic ring as well as to increased yields of
337 carboxylic acids and toxic dicarbonyl compounds (Sun et al., 2010; Yu et al., 2014;
338 Prasse et al., 2018). For example, some highly oxygenated C_2 - C_5 aliphatic
339 compounds (e.g., $C_2H_2O_4$, $C_3H_4O_4$, $C_4H_6O_4$, and $C_5H_6O_5$) corresponding to
340 carboxylic acids (Yu et al., 2014) were clearly observed in the mass spectra of
341 present photochemical products. The presence of these oxygenated products not only

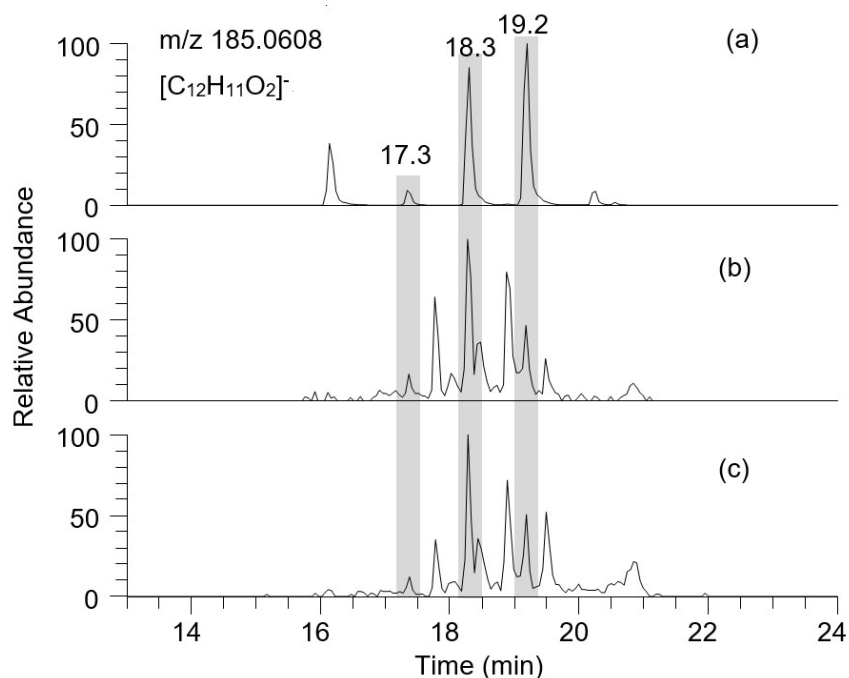


342 directly increased the degree of oxygenation in the bulk solution composition, but
343 also contributed to the variation of solution acidity. The pH measurements indicated
344 that the acidities ($[H^+]$) of the bulk solution increased by $(2.96 \pm 0.15) \times 10^{-5}$ M and
345 $(4.26 \pm 0.16) \times 10^{-5}$ M for phenol and guaiacol, respectively.

346 The oligomerization induced by photochemical transformation of phenolic
347 substances is an important formation pathway for the low-volatility, light-absorbing
348 compounds (Smith et al., 2016). Here, phenolic dimers (i.e., $C_{12}H_{10}O_2$ for phenol
349 dimer and $C_{14}H_{14}O_4$ for guaiacol dimer) and higher oligomers (e.g., $C_{18}H_{14}O_3$ and
350 $C_{24}H_{18}O_4$ for phenol trimer and tetramer, $C_{21}H_{20}O_6$ for guaiacol trimer), as well as
351 their hydroxylated species were observed. The formation mechanism, can be
352 ascribed to C-O or C-C coupling of phenoxy radicals that were formed via
353 H-abstraction of the phenols or OH addition to the aromatic ring (Net et al., 2009,
354 Sun et al, 2010). The reaction at the para position or para-para coupling was more
355 likely to occur due to a higher probability of free electron to occur in this position
356 (Lavi et al, 2017) or a weaker steric hindrance in the para position. The extracted LC
357 diagrams of m/z 185.0608 and 245.0823 are shown in Figure 5a and Figure 6a,
358 respectively, where both ions involve dimers of phenol and guaiacol with several
359 structures, and/or other isomers. The presence of guaiacol dimer and syringol dimer
360 was previously observed in aerosol samples largely affected by wood combustion.
361 Based on the Aerosol Mass Spectrometer (AMS) analysis, these two dimers were
362 suggested as markers of biomass burning aerosols (Sun et al., 2010; Yu et al., 2014).
363 In the composition of present biomass burning aerosols, the phenolic dimers (m/z



364 185.0608 and 245.0823) were also observed in present mass spectra, but the
365 extracted LC diagrams shown in Figure 5b-c and Figure 6b-c indicate that these ions
366 contain multiple RT peaks. The same peaks with RT18.3 and 19.2 min which are
367 assumed to be the phenol dimers were observed during the photochemical
368 transformation of phenol (Figure 5a) and in the straw-burning samples (Figure 5b-c).
369 Meanwhile, the present particle extracts may also involve guaiacol dimer, since its
370 m/z 245.0823 has two LC peaks emerged at RT 17.7 and 19.5 min (Figure 6b-c)
371 same as the peaks identified during the photochemical transformation of guaiacol
372 (Figure 6a).

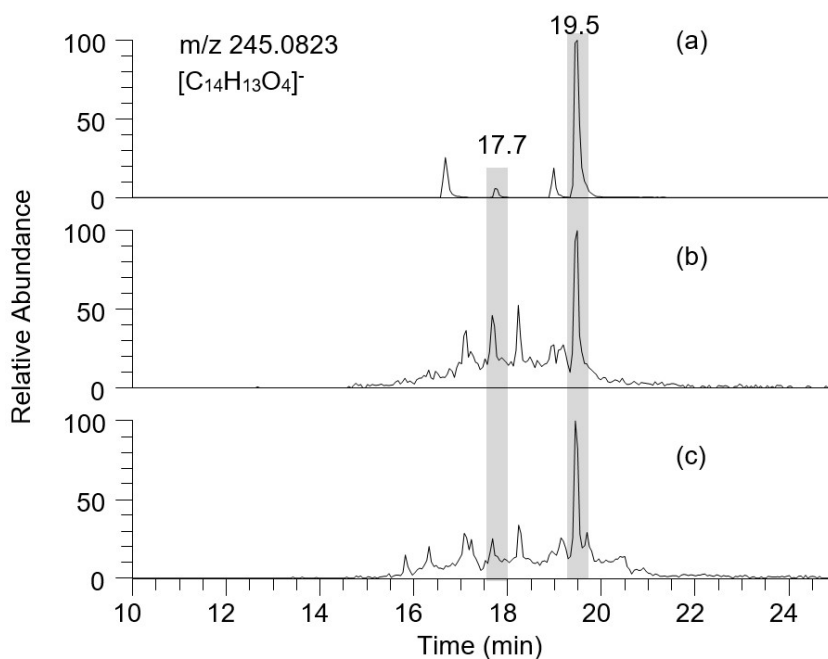


373
374 **Figure 5. Extracted LC chromatograms of m/z 185.0608 in (a) photochemical sample of**
375 **phenol, (b) HNWX-1, and (c) HBDM-2.**
376

377 Typical hydroxylated species such as, e.g., C₂H₂O₄, C₆H₆O₂, C₇H₆O₃, C₇H₈O₃,



378 were also found in the samples emerged from the photooxidation of both phenols
379 and the straw-burning samples. The comparison of the photooxidation products
380 stemmed from the phenols and the straw-burning samples revealed their significant
381 difference, pointing to the importance of studying real aerosol samples against the
382 laboratory model compounds. However, evaluating the model compounds as proxy
383 of real aerosol samples is always helpful as a reference. To this end, it is worth
384 noting that potentially other phenols and methoxyphenols (e.g., acetosyringone,
385 vanillin) that dissolve into cloud, fog droplets or aerosol liquid water can be
386 photochemically transformed and contribute to the SOA formation (Vione et al.,
387 2019, Zhou et al., 2019).



388
389 **Figure 6.** Extracted LC chromatograms of m/z 245.0823 in (a) photochemical sample of
390 guaiacol, (b) HNWX-1, and (c) HBDM-2.

391 **3.3 Photochemistry of aqueous extracts derived from straw burning aerosols**



392 Although the direct photolysis was performed on present straw burning samples in
393 presence of simulated sunlight irradiation without adding any oxidants, the
394 photooxidation process still occurred since the particle extracts were very likely to
395 include various oxidants, e.g., singlet molecular oxygen ($^1\text{O}_2$), peroxides, hydroxyl
396 radical (OH) or excited triplet state of organics produced under light excitation
397 (Anastasio et al., 1997; Vione et al., 2006; Net et al., 2009; Net et al., 2010; Bateman
398 et al., 2011; Rossignol et al., 2014; Smith et al., 2014; Gómez Alvarez et al., 2012).
399 In particular, the excited triplet state of aromatic carbonyls (e.g., 3,
400 4-dimethoxybenzaldehyde) was found to be more efficient than OH radical to
401 oxidize phenols and produce hydroxylated species (Smith et al., 2014., Yu et al.,
402 2014). This photosensitized reaction is likely to play an important role in the WSOC
403 evolution, due to high quantities of aromatic carbonyls present in the extracts of
404 biomass burning aerosols.

405 Although no available standards were utilized for absolute quantification, the
406 variation in peak abundance at unique retention times in the chromatogram could
407 reflect the extent of evolution of WSOC molecules, with accurate molecular weights.
408 The LC/ESI-HRMS monitors changes in the molecular features of a part of the
409 WSOC, i.e., photodegradation of low oxygenated compounds and formation of high
410 oxygenated compounds. Table 1 lists the CHO compounds for which the LC peak
411 intensities significantly increased and decreased after the 12-hour photolysis.

412 **3.3.1 Photodegradation of low oxygenated compounds and formation of highly**
413 **oxygenated compounds**



414 As shown in Table 1, ion masses assigned with high unsaturated and low
415 oxygenated species ($O/C < 0.5$) are prone to photodegradation, especially C_7 - C_9
416 compounds (possible aromatic species), which intensity decreased by nearly one
417 order of magnitude. For example, for m/z 123.0450 ($[C_7H_7O_2]$), as shown in Figure
418 7a, the peaks at RT 16.2 and 16.7 min in the LC chromatogram reduced in area by 95%
419 after the 12-h irradiation. Using a standard it was verified that both peaks did not
420 belong to guaiacol (peak at RT 17.3 min), but they were also found within the
421 products of guaiacol photo-oxidation, suggesting that they might be isomers of
422 guaiacol or aromatic dihydric alcohol.

423 **Table 1. M/Z with significant changes upon 12-h photolysis analyzed by LC/ESI-HRMS.**

Precursor (LC peak intensity decreases by >50%)			Product (LC peak intensity increases by >50%)		
Retention time, min	Measured m/z	Molecular formula	Retention time, min	Measured m/z	Molecular formula
16.2,16.7	123.04497	$C_7H_8O_2$	1.9	59.01362	$C_2H_4O_2$
13.9,14.5	129.05555	$C_6H_{10}O_3$	1.8	72.99291	$C_2H_2O_3$
14.6	131.07121	$C_6H_{12}O_3$	2.1	73.02928	$C_3H_6O_2$
14.6	133.02934	$C_8H_6O_2$	1.8	75.00856	$C_2H_4O_3$
15.9	135.04498	$C_8H_8O_2$	2.4	85.02930	$C_4H_6O_2$
13.7	137.02426	$C_7H_6O_3$	1.9, 4.4	87.04496	$C_4H_8O_2$
17.7	137.06063	$C_8H_{10}O_2$	1.9	88.98785	$C_2H_2O_4$
15.8	147.04504	$C_9H_8O_2$	1.9	89.02427	$C_3H_6O_3$
17.2	149.06062	$C_9H_{10}O_2$	2.2	99.00857	$C_4H_4O_3$
19.0	151.07634	$C_9H_{12}O_2$	2.5	129.01917	$C_5H_6O_4$
16.8	161.06068	$C_{10}H_{10}O_2$	2.0	145.01407	$C_3H_6O_5$
16.2	165.05559	$C_9H_{10}O_3$	1.9	147.02971	$C_3H_8O_5$
14.9	167.07129	$C_9H_{12}O_3$	14.9	155.03482	$C_7H_8O_4$
15.1	181.05048	$C_9H_{10}O_4$	15.1	169.01411	$C_7H_6O_5$
17.3	191.03498	$C_{10}H_8O_4$	16.4	183.02980	$C_8H_8O_5$
16.2	195.06622	$C_{10}H_{12}O_4$			
18.6	207.06635	$C_{11}H_{12}O_4$			



425 The phenolic dimers ($C_{12}H_{10}O_2$ and $C_{14}H_{14}O_4$) as described above also exhibited a
426 decreasing tendency with almost complete disappearance after 12h direct photolysis.
427 Other species with relatively high MW (≥ 200 Da) were also observed to be
428 decomposed, including m/z 251.0564 ($[C_{12}H_{11}O_6]^+$), 313.0724 ($[C_{17}H_{13}O_6]^+$), and
429 329.0674 ($[C_{17}H_{13}O_7]^+$) (Figure S5), although their initial abundance was not very
430 high.

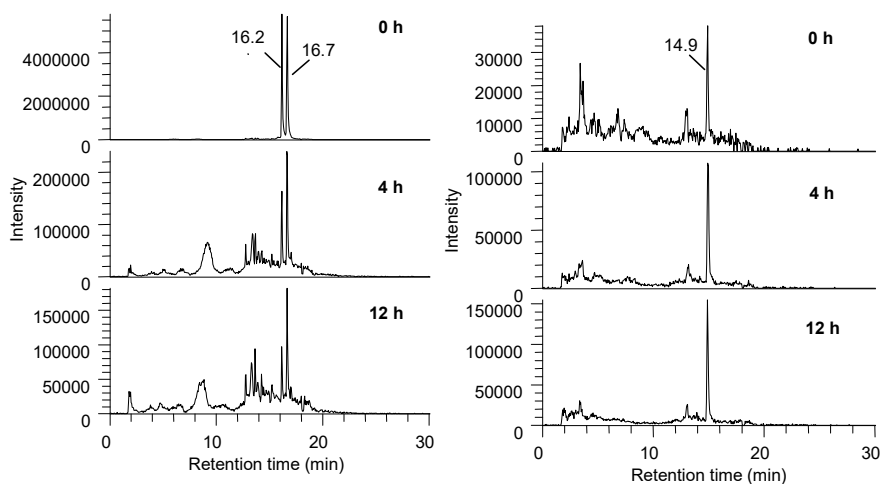
431 On the other hand, the solution acidity ($[H^+]$) of the particle extracts increase after
432 the 12-hour photolysis, similar to the observation on the photo-oxidation of phenols
433 (section 3.2) that resulted in the formation of oxygenated species. The solution
434 acidity ($[H^+]$) normalized by WSOC concentration ($[OC_{ws}]$) was increased with a
435 variation of $\Delta[H^+]/[OC_{ws}]=(3.8 \pm 0.8) \times 10^{-7} \text{ mol mgC}^{-1}$, suggesting the formation of
436 new acidic substances.

437 The photochemical processing has led to an increased formation of low MW
438 compounds (e.g., C_2 - C_5 species), with a relatively high O/C ratio. For example, the
439 C_2 compounds, including $[C_2H_1O_3]^+$, $[C_2H_3O_3]^+$, $[C_2H_3O_2]^+$, and $[C_2H_1O_4]^+$ (Figure
440 S6), which may correspond to glyoxylic acid, glycolic acid, acetic acid, and oxalic
441 acid, respectively, were likely to be formed via oxidation pathway of several
442 water-soluble molecules with photochemical reactivity (e.g., glyoxal (Carlton et al.,
443 2007; Lim et al., 2010), methylglyoxal (Altieri et al., 2008; Lim et al., 2010),
444 pyruvic acid (e.g. Grgic et al., 2010; Griffith et al., 2013; Reed Harris et al., 2014;
445 Rapf et al., 2017; Eugene and Guzman, 2017, Mekic et al., 2018), phenols (Sun et al.,
446 2010), etc). The presence of these highly oxygenated compounds that possibly



447 contain acidic groups (e.g., $-\text{COOH}$ and $-\text{OH}$) undoubtedly contributed to the
448 increase of the solution acidity. Higher levels of other highly oxygenated species
449 such as $[\text{C}_3\text{H}_5\text{O}_3]^-$, $[\text{C}_4\text{H}_7\text{O}_2]^-$, $[\text{C}_5\text{H}_5\text{O}_5]^-$ and $[\text{C}_5\text{H}_7\text{O}_5]^-$ were also observed (Figure
450 S7).

451 To identify the impact of photolysis on the evolution of specific WSOC, the ions
452 of $[\text{C}_7\text{H}_7\text{O}_n]^-$ in the HBDM-1 sample with significant variation were chosen as
453 representative cases for description. The relative intensity of $[\text{C}_7\text{H}_7\text{O}_2]^-$ and
454 $[\text{C}_7\text{H}_7\text{O}_3]^-$ decreased dramatically, while the intensities of $[\text{C}_7\text{H}_7\text{O}_4]^-$, $[\text{C}_7\text{H}_7\text{O}_5]^-$ and
455 $[\text{C}_7\text{H}_7\text{O}_6]^-$ increased with photolysis (Figure 7 just shown the variation of $[\text{C}_7\text{H}_7\text{O}_2]^-$
456 and $[\text{C}_7\text{H}_7\text{O}_4]^-$). It seems reasonable that the possible hydroxylation of $[\text{C}_7\text{H}_7\text{O}_2]^-$ and
457 $[\text{C}_7\text{H}_7\text{O}_3]^-$ might contribute to the formation of $[\text{C}_7\text{H}_7\text{O}_5]^-$ and $[\text{C}_7\text{H}_7\text{O}_6]^-$. Although
458 we could not verify this hypothesis, the formed oxidized species undoubtedly have a
459 high O/C ratio which highlights the possibility of this reaction pathway.



460

461 **Figure 7.** Extracted LC chromatograms from HBDM-2 of (a) $[\text{C}_7\text{H}_7\text{O}_2]^-$ and (b) $[\text{C}_7\text{H}_7\text{O}_4]^-$ at
462 different photolytic stages of 0, 4, and 12 h.



463 3.3.2 Effect of photolytic processing on other WSOC

464 Some of the detected organic species exhibit a good photochemical stability, as
465 their relative intensities only slightly decreased (<10%) after 12h light irradiation.
466 The m/z 161.0454 ($[C_6H_9O_5]^-$) presented two prominent peaks at RT1.9 and 2.4 min
467 (Figure S8). The peak at RT 2.4 min was suggested to be levoglucosan, a typical
468 tracer of biomass burning aerosols (Hu et al., 2013). Its presence in the sample was
469 further confirmed with a standard compound. The relatively good photochemical
470 stability was also observed for some C_6 homolog compounds, such as $[C_6H_7O_6]^-$,
471 $[C_6H_9O_6]^-$, and $[C_6H_{11}O_6]^-$. Some other oxygenated species, such as $[C_3H_3O_3]^-$,
472 $[C_4H_5O_4]^-$, $[C_3H_3O_4]^-$, and $[C_4H_5O_5]^-$ remained relatively stable, as well.

473 Regarding the CHON compounds, only small variation of the chromatogram
474 peaks, was observed for most of the detected species. In particular, several species
475 with low O/C decreased by less than 30%, e.g., m/z 94.0297 ($[C_5H_4ON]^-$, RT 7.1
476 min), and 120.0453 ($[C_7H_6ON]^-$, RT12.2 min). Some compounds were
477 photochemically very stable as the variation of their peak intensities was less than
478 10 % upon light irradiation of the samples, e.g., m/z 118.0297 ($[C_7H_4ON]^-$, RT16.6
479 and 17.1 min), 146.0246 ($[C_8H_4O_2N]^-$, RT14.4 min), and 190.0510 ($[C_{10}H_8O_3N]^-$,
480 RT17.8 min). However, the intensities of the ion masses with relatively higher
481 degree of oxygenation was found to increase substantially (>50%), e.g., m/z
482 162.0195 ($[C_8H_4O_3N]^-$, RT 17.2 min), 198.0408 ($[C_8H_8O_5N]^-$, RT 18.0 min), and
483 242.1763 ($[C_{13}H_{24}O_3N]^-$, RT 17.9 min).

484 Another intriguing finding was that different structural isomers with the same



485 molecular mass might have exhibited different fates upon prolonged light irradiation
486 of the samples. For example, the intensity of the peak at m/z 165.0405 ($[C_5H_9O_6]^+$)
487 decreased when it was eluted at 4.9 min, but increased at RT 1.8 min, with the
488 irradiation time (Figure S9). A simultaneous degradation and formation among
489 isomers of some CHON ion masses upon prolonged light irradiation, was also
490 observed, as was the case for the CHO compounds. For example, the m/z 108.0453
491 assigned to $[C_6H_6ON]^+$, might include hydroxy and amino groups on the phenyl ring
492 to present three possible isomers (Figure S10). During photolytic processing, the
493 intensity of the peak at RT 3.2 min increased dramatically, while there was a clear
494 decreasing tendency of the peak intensity at RT 5.5 and 12.5 min, which was
495 suggestive of possible isomerization among these isomers. Other ion masses that
496 exhibited possible isomerization included m/z 122.0610 ($[C_7H_8ON]^+$), 132.0454
497 ($[C_8H_6ON]^+$), 134.0245 ($[C_7H_4O_2N]^+$), 136.0403 ($[C_7H_6O_2N]^+$), 138.0559
498 ($[C_7H_8O_2N]^+$), 144.0453 ($[C_9H_6ON]^+$), and 152.0352 ($[C_7H_6O_3N]^+$).

499 3.3.3 Effect of photolytic processing on mass spectral features of WSOC

500 Since the LC method just separated a fraction of polar compounds, we tentatively
501 utilized the change of HRMS to gain more comprehensive information about the
502 WSOC evolution. We compared the time-profile (0, 4, and 12h) mass spectra with
503 each other, based on the assumption of same interference from inorganic species, and
504 the good reproducibility and stability for orbitrap MS operated under the same
505 instrumental parameter (the RSD of TIC intensity within 5%). It is well known that
506 ESI mass spectral abundances are influenced by the solution composition,



507 concentration of analytes and instrumental factors (Bateman et al., 2011); hence, it is
508 quite challenging to directly quantify the absolute concentration levels of the
509 complex mixtures. Despite that, the photochemical degradation of WSOC
510 compounds and corresponding formation of organic compounds can be well
511 described by the variation of signal intensity from mass spectrometry. The average
512 O/C and H/C ratios for CHO compounds were from 0.38 ± 0.02 to 0.44 ± 0.02 and
513 1.24 ± 0.03 to 1.26 ± 0.01 , respectively, as the irradiation time extended up to 12h.
514 The comparison of these time-profile mass spectra indicates that the 12-hour
515 photolysis resulted in a significant reduction of $28 \pm 11\%$ in the total ion abundance
516 (S/N). Since the photolysis induced changes in abundance for most of the CHO
517 compounds, we also calculated the intensity (S/N)-weighted average O/C (O/C_w) and
518 H/C (H/C_w) (Bateman et al., 2011; Romonosky et al., 2015) with values ranging
519 from 0.45 ± 0.03 to 0.53 ± 0.06 and from 1.32 ± 0.09 to 1.40 ± 0.11 , respectively.
520 Both average O/C ratios with and without intensity-weighted showed an increased
521 tendency that indicated an elevation in the degree of oxygenation of bulk extract
522 composition, consistent with the LC observation, i.e. formation of highly oxygenated
523 species and the consumption of low oxygenated compounds. This result bears
524 similarity with previous observation using ESI mass spectrometry on characterizing
525 photochemical transformations of d-limonene in the aqueous phase as a source of
526 SOA (Bateman et al., 2011).

527 4 CONCLUSIONS

528 This study was focused on the effect of direct photolysis on the molecular



529 composition of actual WSOC extracted from fresh straw-burning aerosol. The
530 photooxidation of phenols in the aqueous phase under laboratory conditions
531 indicates that the phenols in real biomass burning WSOC would likely have potential
532 to experience the similar evolution to form various oxygenated compounds under
533 relevant cloudwater condition. Because the extract composition was very complex,
534 the high-resolution mass spectrometers used in this study (ESI-HRMS and
535 LC/ESI-HRMS), although advanced still had limitations in monitoring the
536 modification of molecular composition, especially for determining the potential
537 formation of compounds present at low concentrations or compounds that were
538 poorly ionized. However, a series of polar molecules were identified that changed
539 their molecular composition via photochemical evolution. In particular, the
540 degradation of low oxygenated compounds with strong photochemical reactivity and
541 the formation of high oxygenated compounds might directly result in an increasing
542 O/C ratio in WSOC. This finding indicates that the water soluble organic fraction of
543 fresh combustion-derived aerosols have the potential to form more oxidized organic
544 matter, which might partly account for the highly oxygenated nature of atmospheric
545 organic aerosols. High MW ion masses ($MW \geq 300\text{Da}$) typical for oligomers were
546 also found in the degradation products (even some with low abundance). Some CHO
547 and CHON species exhibited no significant losses ($< 10\%$), and displayed good
548 photochemical stability, which indicates that they may also be potential candidates of
549 tracers of biomass burning aerosols.

550 **AUTHOR CONTRIBUTION**



551 Jing Cai and Zhiqiang Yu designed the experiments, and Jing Cai and Xiangying
552 Zeng carried them out. Guorui Zhi provided the straw-burning aerosol samples,
553 Sasho Gligorovski helped perform the analysis of light irradiation. Guoying Sheng,
554 Xinming Wang and Ping'an Peng provided some technical consultations about
555 organic chemistry. Jing Cai prepared the manuscript with contributions from all
556 co-authors.

557 **ACKNOWLEDGMENTS**

558 This study was financially supported by the National Key Technology Research and
559 Development Program of the Ministry of Science and Technology of China
560 (2014BAC22B04), the National Natural Science Funds of China (41225013,
561 41530641, and 41373131) and the Science and Technology Project of Guangdong
562 Province, China (2014B030301060).

563 **REFERENCES**

- 564 Altieri, K. E., Seitzinger, S. P., Carlton, A. G., Turpin, B. J., Klein, G. C. and Marshall, A. G.:
565 Oligomers formed through in-cloud methylglyoxal reactions: Chemical composition, properties,
566 and mechanisms investigated by ultra-high resolution FT-ICR mass spectrometry. *Atmospheric*
567 *Environment*, 42, 1476-1490, 2008.
- 568 Altieri, K. E., Turpin, B. J. and Seitzinger, S. P.: Oligomers, organosulfates, and nitrooxy
569 organosulfates in rainwater identified by ultra-high resolution electrospray ionization FT-ICR
570 mass spectrometry, *Atmospheric Chemistry and Physics*, 9, 2533-2542, 2009a.
- 571 Altieri, K. E., Turpin, B. J. and Seitzinger, S. P.: Composition of Dissolved Organic Nitrogen in
572 Continental Precipitation Investigated by Ultra-High Resolution FT-ICR Mass Spectrometry,
573 *Environmental Science & Technology*, 43, 6950-6955, doi: 10.1021/es9007849, 2009b.
- 574 Anastasio, C., Faust, B. C. and Rao, C. J.: Aromatic carbonyl compounds as aqueous-phase



575 photochemical sources of hydrogen peroxide in acidic sulfate aerosols, fogs, and clouds .1.
576 Non-phenolic methoxybenzaldehydes and methoxyacetophenones with reductants (phenols),
577 Environmental Science & Technology, 31, 218-232, 1997.

578 Bateman, A. P., Nizkorodov, S. A., Laskin, J. and Laskin, A.: Photolytic processing of secondary
579 organic aerosols dissolved in cloud droplets, Physical Chemistry Chemical Physics,13,
580 12199-12212, doi: 10.1039/c1cp20526a, 2011.

581 Boone, E. J., Laskin, A., Laskin, J., Wirth, C., Shepson, P. B., Stirm, B. H. and Pratt, K. A.: Aqueous
582 Processing of Atmospheric Organic Particles in Cloud Water Collected via Aircraft Sampling,
583 Environmental Science & Technology,49, 8523-8530, doi: 10.1021/acs.est.5b01639, 2015.

584 Cai, J., Zhi, G., Yu, Z., Nie, P., Gligorovski, S., Zhang, Y., Zhu, L., Guo, X., Li, P., He, T., He, Y.,
585 Sun, J. and Zhang, Y.: Spectral changes induced by pH variation of aqueous extracts derived
586 from biomass burning aerosols: Under dark and in presence of simulated sunlight irradiation,
587 Atmospheric Environment, 185, 1-6, doi: 10.1016/j.atmosenv.2018.04.037. 2018.

588 Cappiello, A., De Simoni, E., Fiorucci, C., Mangani, F., Palma, P., Trufelli, H., Decesari, S., Facchini,
589 M. C. and Fuzzi, S.: Molecular characterization of the water-soluble organic compounds in
590 fogwater by ESIMS/MS, Environmental Science & Technology, 37, 1229-1240, doi:
591 10.1021/es0259990, 2003.

592 Chang, J. L. and Thompson, J. E.: Characterization of colored products formed during irradiation of
593 aqueous solutions containing H₂O₂ and phenolic compounds, Atmospheric Environment, 44,
594 541-551, doi: 10.1016/j.atmosenv.2009.10.042, 2010.

595 Carlton, A. G., Turpin, B. J., Altieri, K. E., Seitzinger, S., Reff, A., Lim, H-J. and Ervens, B.:
596 Atmospheric oxalic acid and SOA production from glyoxal: Results of aqueous photooxidation
597 experiments. Atmospheric Environment, 41, 7588–7602, 2007.

598 Collett, J.L., Hoag, K.J., Sherman, D.E., Aaron Bator; Richards, W.L. Spatial and temporal variations
599 in San Joaquin Valley fog chemistry, Atmospheric Environment, 33 (1), 129-140, 1998.Daumit,
600 K. E., Carrasquillo, A. J., Hunter, J. F. and Kroll, J. H.: Laboratory studies of the aqueous-phase
601 oxidation of polyols: submicron particles vs. bulk aqueous solution, Atmospheric Chemistry and
602 Physics,14, 10773-10784, doi: 10.5194/acp-14-10773-2014, 2014.

603 Duarte, R. M. B. O., Santos, E. B. H., Pio, C. A. and Duarte, A. C.: Comparison of structural features
604 of water-soluble organic matter from atmospheric aerosols with those of aquatic humic
605 substances, Atmospheric Environment,41, 8100-8113, doi: 10.1016/j.atmosenv.2007.06.034,



- 606 2007.
- 607 Eugene, A. J. and Guzman, M. I. Reactivity of Ketyl and Acetyl Radicals from Direct Solar Actinic
608 Photolysis of Aqueous Pyruvic Acid. *Journal of Physical Chemistry A*, 121, 2924–2935, 2017.
- 609 Fahey, K. M., Pandis, S. N., Collett, J. L. and Herckes, P. The influence of size-dependent droplet
610 composition on pollutant processing by fogs, *Atmospheric Environment*, 39(25), 4561-4574,
611 2005.
- 612 Fine, P. M., Cass, G. R. and Simoneit, B. R. T.: Chemical characterization of fine particle emissions
613 from fireplace combustion of woods grown in the northeastern United States, *Environmental
614 Science & Technology*, 35, 2665-2675, 2001.
- 615 Fu, P. Q., Kawamura, K., Chen, J., Qin, M. Y., Ren, L. J., Sun, Y. L., Wang, Z. F., Barrie, L. A.,
616 Tachibana, E., Ding, A. J. and Yamashita, Y.: Fluorescent water-soluble organic aerosols in the
617 High Arctic atmosphere, *Scientific Reports*, 5, 2015.
- 618 Gilardoni, S., Massoli, P., Paglione, M., Giulianelli, L., Carbone, C., Rinaldi, M., Decesari, S.,
619 Sandrini, S., Costabile, F., Gobbi, G. P., Pietrogrande, M. C., Visentin, M., Scotto, F., Fuzzi, S.
620 and Facchini, M. C.: Direct observation of aqueous secondary organic aerosol from
621 biomass-burning emissions, *Proceedings of the National Academy of Sciences of the United
622 States of America*, 113, 10013-10018, 2016.
- 623 Gómez Alvarez, E., Wortham, H., Strekowski, R., Zetzsch, C., S. Gligorovski, S.: Atmospheric
624 photo-sensitized heterogeneous and multiphase reactions: From outdoors to indoors,
625 *Environmental Science & Technology*, 46, 1955-1963, 2012.
- 626 Graham, B., Mayol-Bracero, O. L., Guyon, P., Roberts, G. C., Decesari, S., Facchini, M. C., Artaxo,
627 P., Maenhaut, W., Koll, P. and Andreae, M. O.: Water-soluble organic compounds in biomass
628 burning aerosols over Amazonia-I. Characterization by NMR and GC-MS, *Journal of
629 Geophysical Research-Atmospheres*, 107, doi: 10.1029/2001jd000336, 2002.
- 630 Grgic, I., Nieto-Gligorovski, L.I., Net, S., Temime-Roussel, B., Gligorovski, S. and Wortham, H.:
631 Light induced multiphase chemistry of gas-phase ozone on aqueous pyruvic and oxalic acids,
632 *Physical Chemistry Chemical Physics*, 12, 698-707, 2010.
- 633 Griffith, E. C., Carpenter, B. K., Shoemaker, R. K. and Vaida, V.: Photochemistry of aqueous pyruvic
634 acid, *Proceedings of the National Academy of Sciences of the United States of America*, 110,
635 11714-11719, doi: 10.1073/pnas.1303206110, 2013.



- 636 Hu, Q., Xie, Z., Wang, X., Hui Kang, H. and Zhang, P.: Levoglucosan indicates high levels of
637 biomass burning aerosols over oceans from the Arctic to Antarctic, *Scientific Reports*, 3, 2013.
- 638 Kitanovski, Z., Cusak, A., Grgic, I. and Claeys, M.: Chemical characterization of the main products
639 formed through aqueous-phase photonitration of guaiacol, *Atmospheric Measurement*
640 *Techniques*, 7, 2457-2470, doi: 10.5194/amt-7-2457-2014, 2014.
- 641 Kroll, J. H., Donahue, N. M., Jimenez, J. L., Kessler, S. H., Canagaratna, M. R., Wilson, K. R., Altieri,
642 K. E., Mazzoleni, L. R., Wozniak, A. S., Bluhm, H., Mysak, E. R., Smith, J. D., Kolb, C. E., and
643 Worsnop, D. R.: Carbon oxidation state as a metric for describing the chemistry of atmospheric
644 organic aerosol, *Nat. Chem. Biol.*, 3, 133–139, 2011.
- 645 Kourtchev, I., Fuller, S., Aalto, J., Ruuskanen, T. M., McLeod, M. W., Maenhaut, W., Jones, R.,
646 Kulmala, M. and Kalberer, M.: Molecular Composition of Boreal Forest Aerosol from Hyttiala,
647 Finland, Using Ultrahigh Resolution Mass Spectrometry, *Environmental Science & Technology*,
648 47, 4069-4079, doi: 10.1021/es3051636, 2013.
- 649 Kourtchev, I., Godoi, R. H. M., Connors, S., Levine, J. G., Archibald, A. T., Godoi, A. F. L., Paralovo,
650 S. L., Barbosa, C. G. G., Souza, R. A. F., Manzi, A. O., Seco, R., Sjostedt, S., Park, J. H., Guenther
651 A., Kim, S., Smith, J., Martin, S. T., and Kalberer, M.: Molecular composition of organic aerosols
652 in central Amazonia: an ultra-high-resolution mass spectrometry study, *Atmospheric Chemistry*
653 *and Physics*, 16, 11899–11913, 2016.
- 654 Krivacsy, Z., Hoffer, A., Sarvari, Z., Temesi, D., Baltensperger, U., Nyeki, S., Weingartner, E.,
655 Kleefeld, S. and Jennings, S. G.: Role of organic and black carbon in the chemical composition
656 of atmospheric aerosol at European background sites, *Atmospheric Environment*, 35, 6231-6244,
657 2001.
- 658 Laskin, A., Smith, J. S. and Laskin, J.: Molecular Characterization of Nitrogen-Containing Organic
659 Compounds in Biomass Burning Aerosols Using High-Resolution Mass Spectrometry,
660 *Environmental Science & Technology*, 43, 3764-3771, doi: 10.1021/es803456n, 2009.
- 661 Lavi, A., Lin, P., Bhaduri, B., Carmieli, R., Laskin, A. and Rudich, Y.: Characterization of light-absorbing
662 oligomers from reactions of phenolic compounds and Fe(III), *Earth and Space Chemistry*, 1,
663 637-646, 2017.
- 664 Lee, A. K. Y., Herckes, P., Leaitch, W. R., Macdonald, A. M. and Abbatt, J. P. D.: Aqueous OH
665 oxidation of ambient organic aerosol and cloud water organics: Formation of highly oxidized



- 666 products, *Geophysical Research Letters*, 38, 2011.
- 667 Lim, Y. B., Tan, Y., Perri, M. J., Seitzinger, S. P. and Turpin, B. J.: Aqueous chemistry and its role in
668 secondary organic aerosol (SOA) formation, *Atmospheric Chemistry and Physics*, 10,
669 10521-10539, doi: 10.5194/acp-10-10521-2010, 2010.
- 670 Lim, Y. B. and Turpin, B. J.: Laboratory evidence of organic peroxide and peroxyhemiacetal
671 formation in the aqueous phase and implications for aqueous OH, *Atmospheric Chemistry and*
672 *Physics*, 15, 12867-12877, doi: 10.5194/acp-15-12867-2015, 2015.
- 673 Lin, P., Rincon, A. G., Kalberer, M. and Yu, J. Z.: Elemental Composition of HULIS in the Pearl
674 River Delta Region, China: Results Inferred from Positive and Negative Electrospray High
675 Resolution Mass Spectrometric Data, *Environmental Science & Technology*, 46, 7454-7462, doi:
676 10.1021/es300285d, 2012a.
- 677 Lin, P., Yu, J. Z., Engling, G. and Kalberer, M.: Organosulfates in Humic-like Substance Fraction
678 Isolated from Aerosols at Seven Locations in East Asia: A Study by Ultra-High-Resolution Mass
679 Spectrometry, *Environmental Science & Technology*, 46, 13118-13127, doi: 10.1021/es303570v,
680 2012b.
- 681 Mayol-Bracero, O. L., Guyon, P., Graham, B., Roberts, G., Andreae, M. O., Decesari, S., Facchini, M.
682 C., Fuzzi, S. and Artaxo, P.: Water-soluble organic compounds in biomass burning aerosols over
683 Amazonia - 2. Apportionment of the chemical composition and importance of the polyacidic
684 fraction, *Journal of Geophysical Research-Atmospheres*, 107, doi: 10.1029/2001jd000522, 2002.
- 685 McNeill, V. F.: Aqueous Organic Chemistry in the Atmosphere: Sources and Chemical Processing of
686 Organic Aerosols, *Environmental Science & Technology*, 49, 1237-1244, 2015.
- 687 Mekic, M., Loisel, G., Zhou, W., Jiang, B., Vione, D., Gligorovski, S.: Ionic strength effects on the
688 reactive uptake of ozone on aqueous pyruvic acid: Implications for air-sea ozone deposition,
689 *Environmental Science and Technology*, 52, 12306–12315, 2018.
- 690 Net, S., Nieto-Gligorovski, L., Gligorovski, S., Temime-Rousell, B., Barbati, S., Lazarou, Y. G., and
691 Wortham, H.: Heterogeneous light induced ozone processing on the organic coatings in the
692 atmosphere, *Atmospheric Environment*, 43, 1683-1692, 2009.
- 693 Net, S., Nieto-Gligorovski, L., Gligorovski, S., and Wortham, H.: Heterogeneous ozonation kinetics of
694 4-phenoxyphenol in presence of photosensitizer, *Atmospheric Chemistry and Physics*, 10,
695 1545-1554, 2010.



- 696 Nguyen, T. B., Lee, P. B., Updyke, K. M., Bones, D. L., Laskin, J., Laskin, A. and Nizkorodov, S. A.:
697 Formation of nitrogen- and sulfur-containing light-absorbing compounds accelerated by
698 evaporation of water from secondary organic aerosols, *Journal of Geophysical*
699 *Research-Atmospheres*, 117, doi: 10.1029/2011jd016944, 2012.
- 700 Ofner, J., Krueger, H. U., Grothe, H., Schmitt-Kopplin, P., Whitmore, K. and Zetzsch, C.:
701 Physico-chemical characterization of SOA derived from catechol and guaiacol - a model
702 substance for the aromatic fraction of atmospheric HULIS, *Atmospheric Chemistry and Physics*,
703 11, 1-15, doi: 10.5194/acp-11-1-2011, 2011.
- 704 Petzold, A., Kopp, C., Niessner, R., 1997. The dependence of the specific attenuation cross-section on
705 black carbon mass fraction and particle size. *Atmospheric Environment*, 31, 661-672, 1997.
- 706 Prasse, C., Ford, B., Nomura, D.K. and Sedlak, D.L.: Unexpected transformation of dissolved phenols
707 to toxic dicarbonyls by hydroxyl radicals and UV light, <https://doi.org/10.1073/pnas.1715821115>,
708 2018.
- 709 Rapf, R. J., Perkins, R. J., Carpenter, B. K. and Vaida, V.: Mechanistic Description of Photochemical
710 Oligomer Formation from Aqueous Pyruvic Acid. *Journal of Physical Chemistry A*, 121,
711 4272–4282, 2017.
- 712 Reed Harris, A. E., Ervens, B., Shoemaker, R. K., Kroll, J. A., Rapf, R. J., Griffith, E. C., Monod, A.,
713 Vaida, V.: Photochemical kinetics of pyruvic acid in aqueous solution. *Journal of Physical*
714 *ChemistryA*, 118 (37), 8505–8516, 2014.
- 715 Romonosky, D. E., Laskin, A., Laskin, J. and Nizkorodov, S. A.: High-Resolution Mass Spectrometry
716 and Molecular Characterization of Aqueous Photochemistry Products of Common Types of
717 Secondary Organic Aerosols, *Journal of Physical Chemistry A*, 119, 2594-2606, doi:
718 10.1021/jp509476r, 2015.
- 719 Rossignol, S., Aregahegn, K. Z., Tinel, L., Fine, L., Noziere, B. and George, C.: Glyoxal Induced
720 Atmospheric Photosensitized Chemistry Leading to Organic Aerosol Growth, *Environmental*
721 *Science & Technology*, 48, 3218-3227, 2014.
- 722 Simoneit, B. R. T.: Biomass burning - A review of organic tracers for smoke from incomplete
723 combustion, *Applied Geochemistry*, 17, 129-162, doi: 10.1016/s0883-2927(01)00061-0, 2002.
- 724 Smith, J. D., Sio, V., Yu, L., Zhang, Q. and Anastasio, C.: Secondary Organic Aerosol Production
725 from Aqueous Reactions of Atmospheric Phenols with an Organic Triplet Excited State,



- 726 Environmental Science & Technology,48, 1049-1057, doi: 10.1021/es4045715, 2014.
- 727 Smith, J. S., Laskin, A. and Laskin, J.: Molecular Characterization of Biomass Burning Aerosols
728 Using High-Resolution Mass Spectrometry, Analytical Chemistry,81, 1512-1521, doi:
729 10.1021/ac8020664, 2009.
- 730 Smith, J. D., Kinney, H. and Anastasio, C.:Phenolic carbonyls undergo rapid aqueous
731 photodegradation to form low-volatility, light-absorbing products,Atmospheric environment, 126,
732 36-44, 2015.
- 733 Sun, Y. L., Zhang, Q., Anastasio, C. and Sun, J.: Insights into secondary organic aerosol formed via
734 aqueous-phase reactions of phenolic compounds based on high resolution mass spectrometry,
735 Atmospheric Chemistry and Physics, 10, 4809-4822, doi: 10.5194/acp-10-4809-2010, 2010.
- 736 Surratt, J. D., Gomez-Gonzalez, Y., Chan, A. W. H., Vermeylen, R., Shahgholi, M., Kleindienst, T. E.,
737 Edney, E. O., Offenberg, J. H., Lewandowski, M., Jaoui, M., Maenhaut, W., Claeys, M., Flagan,
738 R. C. and Seinfeld, J. H.: Organosulfate formation in biogenic secondary organic aerosol, Journal
739 of Physical Chemistry A, 112, 8345-8378, doi: 10.1021/jp802310p, 2008.
- 740 Surratt, J. D., Kroll, J. H., Kleindienst, T. E., Edney, E. O., Claeys, M., Sorooshian, A., Ng, N. L.,
741 Offenberg, J. H., Lewandowski, M., Jaoui, M., Flagan, R. C. and Seinfeld, J. H.: Evidence for
742 organosulfates in secondary organic aerosol, Environmental Science & Technology,41, 517-527,
743 doi: 10.1021/es062081q, 2007.
- 744 Tong, H., Kourtchev, I., Pant, P., Keyte, I. J., O'Connor, I. P., Wenger, J. C., Pope, F. D., Harrison, R.
745 M. and Kalberer, M.: Molecular composition of organic aerosols at urban background and road
746 tunnel sites using ultra-high resolution mass spectrometry. Faraday Discussions, 189, 51–68,
747 2016.
- 748 Vione, D., Maurino, V., Minero, C., Pelizzetti, E., Harrison, M. A. J., Olariu, R. I. and Arsene, C.:
749 Photochemical reactions in the tropospheric aqueous phase and on particulate matter, Chemical
750 Society Reviews, 35, 441-453, 2006.
- 751 Vione, V., Albinet, A., Barsotti, F.,Mekic,M., Jiang, B.,Minero, C.,Brigante, M.,Gligorovski, S.:
752 Formation of substances with humic-like fluorescence properties, upon photoinduced
753 oligomerization of typical phenolic compounds emitted by biomass burning, Atmospheric
754 Environment, <https://doi.org/10.1016/j.atmosenv.2019.03.005>,2019.
- 755 Wang, X. K., Rossignol, S., Ma, Y., Yao, L., Wang, M. Y., Chen, J. M., George, C. and Wang, L.:



- 756 Molecular characterization of atmospheric particulate organosulfates in three megacities at the
757 middle and lower reaches of the Yangtze River, *Atmospheric Chemistry and Physics*, 16,
758 2285-2298, 2016.
- 759 Wang, X., Hayeck, N., Brüggemann, M., Yao, L., Chen, H., Zhang, C., Emmelin, C., Jianmin Chen, J.,
760 George, C. and Lin Wang, L. Chemical characteristics of organic aerosols in shanghai: A study
761 by ultrahigh-performance liquid chromatography coupled with Orbitrap mass spectrometry,
762 *Journal of Geophysical Research-Atmospheres*, 122 (11), 703–722, 2017.
- 763 Wozniak, A. S., Bauer, J. E., Sleighter, R. L., Dickhut, R. M. and Hatcher, P. G.: Technical Note:
764 Molecular characterization of aerosol-derived water soluble organic carbon using ultrahigh
765 resolution electrospray ionization Fourier transform ion cyclotron resonance mass spectrometry,
766 *Atmospheric Chemistry and Physics*, 8, 5099-5111, 2008.
- 767 Xie, M. J., Mladenov, N., Williams, M. W., Neff, J. C., Wasswa, J. and Hannigan, M. P.: Water soluble
768 organic aerosols in the Colorado Rocky Mountains, USA: composition, sources and optical
769 properties, *Scientific Reports*, 6, 2016.
- 770 Yee, L. D., Kautzman, K. E., Loza, C. L., Schilling, K. A., Coggon, M. M., Chhabra, P. S., Chan, M.
771 N., Chan, A. W. H., Hersey, S. P., Crouse, J. D., Wennberg, P. O., Flagan, R. C. and Seinfeld, J.
772 H.: Secondary organic aerosol formation from biomass burning intermediates: phenol and
773 methoxyphenols, *Atmospheric Chemistry and Physics*, 13, 8019-8043, 2013.
- 774 Yu, L., Smith, J., Laskin, A., Anastasio, C., Laskin, J. and Zhang, Q.: Chemical characterization of
775 SOA formed from aqueous-phase reactions of phenols with the triplet excited state of carbonyl
776 and hydroxyl radical, *Atmospheric Chemistry and Physics*, 14, 13801-13816, doi:
777 10.5194/acp-14-13801-2014, 2014.
- 778 Zhao, Y., Hallar, A. G. and Mazzoleni, L. R.: Atmospheric organic matter in clouds: exact masses and
779 molecular formula identification using ultrahigh-resolution FT-ICR mass spectrometry,
780 *Atmospheric Chemistry and Physics*, 13, 12343-12362, doi: 10.5194/acp-13-12343-2013, 2013.
- 781 Zhi, G., Chen, Y., Xue, Z., Meng, F., Cai, J., Sheng, G. and Fu, J.: Comparison of elemental and black
782 carbon measurements during normal and heavy haze periods: implications for research,
783 *Environmental Monitoring and Assessment*, 186, 6097-6106, doi: 10.1007/s10661-014-3842-2,
784 2014.
- 785 Zhou, W., Mekic, M., Liu, J., Loisel, G., Jin, B., Vione, D., Gligorovski, S.: Ionic strength effects on



- 786 the photochemical degradation of acetosyringone in atmospheric deliquescent aerosol particles,
787 Atmospheric Environment, 198, 83-88, 2019.